

EXPRESS LETTER

Non-chondritic oxygen isotopic component of metals in a noble-gas-rich chondrite —vestige of stellar wind from the protosun?

KUMIKO FUJIMOTO,¹ SHOICHI ITOH,¹ SHINGO EBATA¹ and HISAYOSHI YURIMOTO^{1,2*}

¹Department of Natural History Sciences, Hokkaido University, Sapporo 060-0810, Japan

²Isotope Imaging Laboratory, Creative Research Institution “Sousei,” Hokkaido University, Sapporo 001-0021, Japan

(Received May 28, 2009; Accepted August 24, 2009; Online published August 28, 2009)

Oxygen isotopic compositions of metal grains in a noble-gas-rich chondrite, NWA 801 CR2, have been determined by secondary ion mass spectrometry. The results show bimodal distribution on $\Delta^{17}\text{O}$ histogram with peaks of $\Delta^{17}\text{O} = 2.3$ and -35.0% . The ^{16}O -rich peak seems to be due to stellar wind from the protosun. The ^{16}O enrichment is comparable with the most ^{16}O -rich value from chondrite constituents. Difference of oxygen isotopic composition of stellar wind between protosun and the present sun implies how self-pollution by planetary embryos during the planet formation epoch have occurred and whether the present solar photosphere preserves the representative composition of the solar system.

Keywords: oxygen isotopes, chondrite, protosun, solar wind, solar system

INTRODUCTION

Oxygen isotopic composition of solar wind from Sun has been determined from lunar metals (Hashizume and Chaussidon, 2005, 2009; Ireland *et al.*, 2006). Recently, NASA's Genesis mission has provided new measurements of solar wind for the present Sun (McKeegan *et al.*, 2009). These data clarified that the Sun has a very different oxygen isotopic composition than the earth, planets and meteorites. However, the solar value is still controversial because the observed isotopic compositions of the Sun are concentrated into two end members, which are enriched or depleted in ^{16}O (60–70%) relative to terrestrial and planetary compositions.

The solar value is generally believed to be representative of the solar system because greater than 99% of the mass of the solar system has been concentrated in the Sun. However, self-pollution of the convective zone of the Sun might have occurred via the infall of planetary embryos during the planet formation epoch of the early solar system (Gonzalez, 1997) because the solar photospheric composition is enriched in metallicity relative to nearby Galactic neighbors (Snow and Witt, 1996). The inferred mass of the convective zone of the present Sun is to be 0.025 solar mass which is roughly comparable with the minimum mass solar nebula.

Oxygen isotopic compositions of planetary embryos are close to the terrestrial value (Yurimoto *et al.*, 2007). This means that the oxygen isotopic composition of the solar photosphere may not be representative of the solar system, and the interior of the Sun should be more enriched in ^{16}O than the convective zone if self-pollution occurred. Furthermore, the oxygen isotopic composition of the solar photosphere would change more ^{16}O -rich with time because the metal-rich convective zone would be diluted by deeper layers with solar evolution (Gonzalez, 1997). This self-pollution model of the solar system can be tested if we determine oxygen isotopic compositions of the solar photosphere during the planet formation epoch, i.e., protosun. Here we report oxygen isotopic compositions of metals in a noble-gas-rich chondrite, which imply vestige of stellar wind from the protosun during the planet formation epoch.

SAMPLES AND METHODS

We studied the NWA 801 carbonaceous chondrite, which is extremely enriched in noble gases of solar origin (Matsuda *et al.*, 2009; Nakashima *et al.*, 2009a, b). Although solar wind normally penetrate less than $1\ \mu\text{m}$ in depth from surface of exposed grains, the solar noble gases in the chondrite are observed in the chondrule interiors and in matrices, which trap the gases with concentration of up to about 10^{-6} and $10^{-4}\ \text{cm}^3\text{STP/g}$ for ^{20}Ne in the chondrules and matrices, respectively. This is the first carbonaceous chondrite observed such noble gas charac-

*Corresponding author (e-mail: yuri@ep.sci.hokudai.ac.jp)

Table 1. Oxygen isotopic and chemical compositions of oxygen-rich inclusions in metal grains of the NWA 801 CR chondrite

$\delta^{17}\text{O}$ (‰)	σ_{mean}	$\delta^{18}\text{O}$ (‰)	σ_{mean}	$\Delta^{17}\text{O}$ (‰)	σ_{mean}	Concentration (ppma)
Metal #24 (in porphyritic olivine pyroxene (POP) type 1 chondrule)						
12.3	6.9	26.7	3.5	-1.6	7.1	306
8.9	8.3	14.4	5.4	1.4	8.8	233
Metal #4 (in matrix)						
12.9	11.0	12.3	6.9	6.5	11.5	61
-2.4	17.5	-6.0	10.9	0.8	18.4	12
Metal #25 (in POP type 1 chondrule rim)						
19.3	11.7	41.8	6.9	-2.5	12.2	75
5.8	10.6	21.3	6.5	-5.3	11.1	29
16.7	9.9	39.1	5.9	-3.7	10.3	216
25.1	13.4	52.9	16.8	-2.4	16.0	79

teristics. Similar noble gas characteristics have been observed in an enstatite chondrite (Okazaki *et al.*, 2001).

A polished thin section of primitive carbonaceous chondrite NWA 801 CR2 was prepared for this study. The thin section was coated by a carbon evaporation film of about 30 nm thick in order to reduce electrostatic charging during high-energy electron and ion bombardments for chemical and isotopic analyses. A field-emission type scanning electron microscope (FE-SEM, JEOL JSM-7000F) equipped with an energy dispersive X-ray spectrometer (EDS, Oxford INCA Energy) has been used to analyze petrographical and surface textures and chemical compositions before and after oxygen isotope analyses.

A secondary ion mass spectrometer (Cameca ims-1270) of Hokkaido University has been used to determine oxygen isotopic compositions in metal grains in the chondrite. A flat-topped and oval-shaped Cs^+ primary beam ($\sim 60 \mu\text{m} \times 100 \mu\text{m}$ in axes) of 20 keV was irradiated on the sample surface with a beam current of ~ 8 nA. Secondary ions emitted from $15 \mu\text{m}$ square at the center of the sputtering crater are detected using a field aperture in order to reduce artifacts from oxygen contaminations on the surface such as adsorbed water.

We measured oxygen isotopic compositions of metals close to surfaces of chondrules and in matrices because solar origin noble gases are observed in chondrule interiors. The measurement positions in metals in chondrules and in matrices were typically about 50–200 μm inside and 50–100 μm inside from the chondrule surface and from the metal surface, respectively.

Because oxygen concentration in metals is extremely low, secondary ions of migrated water from an adsorbed water layer on the surface and of adsorbed water from residual gas in the vacuum chamber cause severe problems to measure intrinsic oxygen in metals. We maintained

the standard and thin section samples in ultra high vacuum (10^{-8} Torr) more than 10 days to evaporate adsorbed water and directly introduced the sample into the analysis chamber. The vacuum of the sample chamber was maintained to $\sim 1 \times 10^{-9}$ Torr and a liquid nitrogen cold-trap was used. Mass resolution of $M/\Delta M \sim 9000$ for 10% valley was applied to reduce contributions of $^{16}\text{OH}^-$ peak. As a result, the contributions of $^{16}\text{OH}^-$ interferences were less than the 2‰ level of ^{17}O intensities although the $^{16}\text{OH}^-$ peak was about three orders of magnitude larger than the ^{17}O peak.

We removed surface contamination layers introduced during polishing of the thin section by sputtering and checked inclusions by monitoring of $^{16}\text{O}^-$ ion projection image of the sputtering surface. After removal of contamination layers, secondary ions of $^{16}\text{O}^-$ -tail, $^{16}\text{O}^-$, $^{17}\text{O}^-$, $^{16}\text{OH}^-$, and $^{18}\text{O}^-$ were sequentially measured for 5, 1, 20, 2, and 10 seconds, respectively, by an electron multiplier (background noise: 0.02 cps) under peak jumping mode. This sequence was cycled 60 times to accumulate ion counts. The $^{16}\text{OH}^-$ contribution to $^{17}\text{O}^-$ peak was corrected by the measurement of $^{16}\text{OH}^-$ -tail assuming similar figures in peak shapes. The correction was less than 2‰ of ^{17}O intensity.

The total measurement time including contamination-layer removal for one analytical spot was about one hour and the sputtered depth of the crater was about 1 μm . The NIST 665 metal standard was used to normalize secondary ion-ratios to $\delta^{17,18}\text{O}$ -values. Analytical precisions are determined by count statistics because of the low count rates of secondary ions, e.g., $^{17}\text{O} = \sim 2$ counts/second. Isotope ratios tested by the standard were reproducible within the count statistics under ranges of secondary ion intensities used in this study.

Oxygen concentrations were calculated by secondary ion intensity ratios between sample and standard assum-

ing linear relationships between concentrations and intensities. We used spinel for the standard and did not include matrix effect corrections because we have no appropriate metal standards for oxygen content analysis. The calibration applied to the NIST 665 metal. The NIST 665 metal contains many oxygen-rich inclusions. The calculated contents of oxygen range from 5 ppma (in inclusion-free area) to 250 ppma (in inclusion-rich area). The large variation is due to the oxygen-rich inclusions of tens- to sub- micrometer sizes scattered in the standard. The reported (not certificated) value of oxygen in the standard is 220 ppma or less (Reed, 1991). Therefore, the absolute concentrations may have systematic errors of a factor of several. On the other hand, the random error is estimated to be less than 30% relative to the concentration by count statistics.

RESULTS AND DISCUSSION

In the metal grains of NWA 801 chondrite, oxide inclusions less than $1 \mu\text{m}$ are common. Characteristic X-ray signals of Mg have not been observed from the inclusions, but Si and O signals have been observed, and a sulfide phase coexists in most cases. The chemical compositions show the oxide inclusions are different from chondrule melt, indicating direct segregation from metal. Oxygen ion intensities from metals containing the inclusions were primarily from the inclusions. The oxygen isotopic compositions lie along the terrestrial fractionation line (Table 1, Fig. 1a) indicating that the metals formed with planetary oxygen isotopic compositions.

After the inclusion segregation, oxygen contents solved in the metals would significantly decrease. Therefore, the metal is a good target to determine trapped oxygen of stellar winds during the planet formation epoch. We selected inclusion-free areas in the metals and analyzed the oxygen isotopes (Fig. 1b). The oxygen isotopic compositions from metals without inclusions mainly plot around the terrestrial fractionation line, but several analyses clearly deviate downward from the terrestrial fractionation line and seem to be large mass fractionation signatures (Table 2, Fig. 1a). In order to clarify the deviation from the terrestrial fractionation line, we introduce $\Delta^{17}\text{O}$ (Fig. 1c).

The histogram of $\Delta^{17}\text{O}$ is composed of two Gaussian curves (Fig. 1c). The main peak curve consists of $\Delta^{17}\text{O} = 2.3\text{‰}$ for the peak and $\pm 7.5\text{‰}$ for the standard deviation. This curve is probably due to terrestrial adsorbed water or to oxide inclusions $\ll 0.1 \mu\text{m}$ because these contributions cannot be completely removed during the experiments.

On the other hand, the accompanying curve consists of $\Delta^{17}\text{O} = -35.0\text{‰}$ for the peak and $\pm 7.1\text{‰}$ for the standard deviation. The oxygen contents are less than 10 ppma

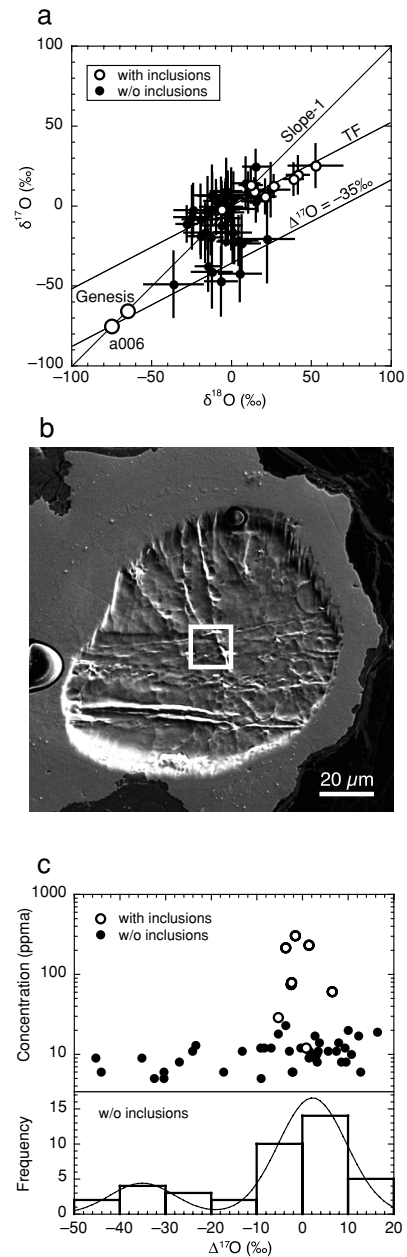


Fig. 1. Oxygen isotopic compositions of metal grains in a gas-rich chondrite, NWA 801 CR2. (a) Three oxygen isotope diagram. Genesis, and a006 correspond to representative oxygen isotopic compositions for solar wind by NASA Genesis mission (Mckeegan et al., 2009), and a chondrite with the most ^{16}O -rich composition (Kobayashi et al., 2003) ever found, respectively. $\delta^{17,18}\text{O} = [(^{17,18}\text{O}/^{16}\text{O})_{\text{metal}} / (^{17,18}\text{O}/^{16}\text{O})_{\text{standard}} - 1] \times 1000$ where the standard is the NIST 665 metal. $\Delta^{17}\text{O} = \delta^{17}\text{O} - 0.52\delta^{18}\text{O}$. Error bars correspond to one standard deviation. (b) A secondary electron image of a metal surface after analysis. Oxygen isotopes from the white square at the center of a sputtering crater were analyzed. The depth of the crater is $\sim 1 \mu\text{m}$. (c) Oxygen concentrations and histogram of metals versus $\Delta^{17}\text{O}$. The histogram can be interpreted by two Gaussian curves characterized by the solar and planetary oxygen isotopic compositions.

Table 2. Oxygen isotopic and chemical compositions of metal grains in the NWA 801 CR chondrite

$\delta^{17}\text{O}$ (‰)	σ_{mean}	$\delta^{18}\text{O}$ (‰)	σ_{mean}	$\Delta^{17}\text{O}$ (‰)	σ_{mean}	Concentration (ppma)
Metal #1 (in porphyritic olivine (PO) type 1 chondrule)						
10.0	16.7	24.8	11.6	-2.9	17.8	11
-19.0	13.7	-19.0	8.4	-9.2	14.4	12
-7.8	14.7	-1.9	7.3	-6.9	15.2	12
-22.4	13.6	1.9	10.3	-23.4	14.6	13
-12.3	24.7	-6.0	12.6	-9.1	25.6	5
-16.8	18.7	1.0	11.3	-17.3	19.6	6
8.3	12.5	10.7	7.4	2.7	13.1	17
Metal #8 (in matrix)						
5.8	11.9	-2.9	10.1	7.4	13.0	11
-4.5	22.4	-14.7	12.9	3.2	23.4	8
8.6	12.5	-2.6	6.8	10.0	13.0	20
24.4	10.5	15.4	7.8	16.4	11.3	19
4.5	16.3	1.4	8.0	3.7	16.8	14
5.0	8.5	16.6	6.6	-3.7	9.2	23
-7.2	19.6	-24.5	11.1	5.6	20.5	11
Metal #15 (in matrix)						
-21.8	15.2	4.5	12.0	-24.1	16.4	11
Metal #17 (in POP type 1 chondrule rim)						
-16.8	18.3	-16.3	13.0	-8.4	19.5	12
-42.5	17.2	5.5	13.1	-45.3	18.5	9
-37.9	15.3	-14.4	7.8	-30.4	15.8	6
6.2	14.1	-11.9	8.5	12.3	14.8	17
Metal #26 (in POP type 1 chondrule rim)						
-20.8	27.1	22.5	16.8	-32.5	28.5	5
-3.3	14.4	-9.3	7.9	1.5	14.9	11
-8.5	21.6	-19.1	11.2	1.4	22.4	9
14.0	16.2	9.1	8.7	9.3	16.8	12
Metal #27 (in POP type 1 chondrule rim)						
-2.0	25.3	0.1	14.8	-2.1	26.4	6
-2.8	16.5	-23.7	11.7	9.5	17.6	8
1.5	12.8	-3.7	6.2	3.4	13.2	11
-19.8	10.6	-12.7	7.3	-13.2	11.2	11
-11.4	11.0	-27.8	6.4	3.1	11.5	10
3.0	13.0	-9.5	7.3	7.9	13.6	14
Metal #31 (in POP type 1 chondrule rim)						
6.8	14.7	-3.1	11.0	8.5	15.7	8
-41.4	22.3	-12.0	12.5	-35.2	23.2	9
9.1	20.2	-3.1	9.6	10.7	20.8	10
6.5	18.5	-12.0	11.5	12.7	19.4	6
Metal #32 (in POP type 1 chondrule rim)						
-0.6	18.2	-6.3	13.1	2.7	19.5	9
-4.1	20.7	-3.5	11.1	-2.3	21.5	6
Metal #34 (in POP type 1 chondrule rim)						
-23.6	17.5	6.6	11.4	-27.0	18.5	8
-47.3	21.4	-6.3	9.9	-44.1	22.0	6
Metal #36 (in POP type 1 chondrule rim)						
-49.1	20.5	-36.1	18.3	-30.4	22.6	5
-1.5	22.8	-2.1	12.4	-0.4	23.7	12
2.8	12.7	15.5	8.4	-5.3	13.4	18

(Fig. 1c). The ^{16}O -rich characteristics are difficult to consider due to analytical artifacts because we have many data of the main peak having the comparable low O concentration level to the ^{16}O -rich data. The mass dependent fractionation trend for ^{16}O -rich data resemble to the data by Hashizume and Chaussidon (2005). The parts per million concentration level is expected for solar origin oxygen in this chondrite based on the noble gas contents of the chondrite and the chondrules (10^{-6} and 10^{-4} cm³STP/g for ^{20}Ne) (Matsuda *et al.*, 2009; Nakashima *et al.*, 2009a, b) and assuming solar abundance of elements ($^{16}\text{O}/^{20}\text{Ne} \sim 7.1$) (Lodders, 2003). These results have the consequence that the accompanying curve consists of trapped stellar winds from the protosun during the planet formation epoch. Energetic solar flare particles of active protosun may be available for the trapping mechanism of stellar wind into chondrule interiors (Okazaki *et al.*, 2001) although further study would be necessary. Therefore, the oxygen isotopic composition of the protosun seems to be enriched in ^{16}O and calculated to be $\Delta^{17}\text{O} = -35.0 \pm 2.1\%$ where the error is standard deviation of the mean. The composition quantitatively agrees with the value of the most ^{16}O -rich composition from meteorites (Kobayashi *et al.*, 2003) and of Hashizume and Chaussidon (2009) and McKeegan *et al.* (2009).

Because there are two possibilities of oxygen isotopic composition of the present solar photosphere, we can develop two scenarios for self-pollution by planetary embryos. If the present solar photosphere is extremely depleted in ^{16}O as shown in Ireland *et al.* (2006), self-pollution by planetary embryos was important process during the planet formation epoch in the solar system. The oxygen isotopic composition of planetary embryos should be extremely depleted in ^{16}O comparing with the Earth. Such ^{16}O -poor compositions are inferred in comets and gas planets (Yurimoto and Kuramoto, 2004; Kuramoto and Yurimoto, 2005).

If the present solar photosphere is enriched in ^{16}O as shown in Hashizume and Chaussidon (2009) and McKeegan *et al.* (2009), the agreement of oxygen isotopic compositions between the protosun and present day sun demonstrate that self-pollution by planetary embryos was not significant for solar system evolution and that the solar photosphere has the representative composition of the solar system.

Acknowledgments—We thank J. Greenwood and K. McKeegan for helpful comments. We thank T. Ireland and an anonymous reviewer for constructive comments and K. Terada for impartial editorial handing. This work was supported by Monka-sho grants.

REFERENCES

- Gonzalez, G. (1997) The stellar metallicity-giant planet connection. *Mon. Not. R. Astron. Soc.* **285**, 403–412.
- Hashizume, K. and Chaussidon, M. (2005) A non-terrestrial ^{16}O -rich isotopic composition for the protosolar nebula. *Nature* **434**, 619–622.
- Hashizume, K. and Chaussidon, M. (2009) Two oxygen isotopic components with extra-selenial origins observed among lunar metallic grains—In search for the solar wind component. *Geochim. Cosmochim. Acta* **73**, 3038–3054.
- Ireland, T. R., Holden, P., Norman, M. D. and Clarke, J. (2006) Isotopic enhancements of ^{17}O and ^{18}O from solar wind particles in the lunar regolith. *Nature* **440**, 776–778.
- Kobayashi, S., Imai, H. and Yurimoto, H. (2003) New extreme ^{16}O -rich reservoir in the early solar system. *Geochem. J.* **37**, 663–669.
- Kuramoto, K. and Yurimoto, H. (2005) Oxygen isotopic heterogeneity in the solar system: the molecular cloud origin hypothesis and its implications for meteorites and the planets. *Chondrites and the Protoplanetary Disk*, Vol. 341 (Krot, A. N., Scott, E. R. D. and Reipurth, B., eds.), 181–192, ASP Conference Series.
- Lodders, K. (2003) Solar system abundances and condensation temperatures of the elements. *Astrophys. J.* **591**, 1220–1247.
- Matsuda, S., Nakashima, D., Iio, H., Bajo, K. and Nagao, K. (2009) Laser microprobe noble gas analysis of chondrules in the NWA 801 CR2 chondrite. *Lunar Planet. Sci.* **XL**, abstract #1628.
- McKeegan, K. D., Kallio, A. P., Heber, V., Jarzebinski, G., Mao, P. H., Coath, C. D., Kunihiro, T., Wiens, R., Allton, J. and Burnett, D. S. (2009) Oxygen isotopes in a Genesis concentrator sample. *Lunar Planet. Sci.* **XL**, abstract #2494.
- Nakashima, D., Matsuda, S., Iio, H., Bajo, K., Ebisawa, N. and Nagao, K. (2009a) Noble gases in the NWA 852/801 CR2 chondrites. *Lunar Planet. Sci.* **XL**, abstract #1661.
- Nakashima, D., Matsuda, S., Iio, H., Bajo, K. and Nagao, K. (2009b) Solar wind like noble gases in a chondrule in the NWA 852 CR2 chondrite. *Lunar Planet. Sci.* **XL**, abstract #1674.
- Okazaki, R., Takaoka, N., Nagao, K., Sekiya, M. and Nakamura, T. (2001) Noble-gas-rich chondrules in an enstatite meteorite. *Nature* **412**, 795–798.
- Reed, W. P. (1991) National Institute of Standards and Technology Certificate of Analysis Standard Reference Material 665. Available at https://www-s.nist.gov/srmors/view_cert.cfm?srm=665
- Snow, T. P. and Witt, A. N. (1996) Interstellar depletions updated: Where all the atoms went. *Astrophys. J.* **468**, L65–L68.
- Yurimoto, H. and Kuramoto, K. (2004) Molecular cloud origin for the oxygen isotope heterogeneity in the solar system. *Science* **305**, 1763–1766.
- Yurimoto, H., Kuramoto, K., Krot, A. N., Scott, E. R. D., Cuzzi, J. N., Thiemens, M. H. and Lyons, J. R. (2007) Origin and Evolution of oxygen isotopic compositions of the solar system. *Protostars and Planets V* (Reipurth, B., Jewitt, D. and Keil, K., eds.), 849–862, University of Arizona Press.